PHYSICAL REVIEW E VOLUME 61, NUMBER 3 MARCH 2000

Oscillations and chaos in catalytic reactions on the nm scale

V. P. Zhdanov[1,2] and B. Kasemo[1]
[1]*Department of Applied Physics, Chalmers University of Technology, S-412 96 Göteborg, Sweden*
[2]*Boreskov Institute of Catalysis, Russian Academy of Sciences, Novosibirsk 630090, Russia*
(Received 24 September 1999)

We present Monte Carlo kinetics of the $2A+B_2 \rightarrow 2AB$ reaction occurring on a 20–30-nm-sized crystallite in the case when reactant adsorption on one of its facets results in surface restructuring. The latter is described on the basis of the well-defined lattice-gas model predicting phase separation in the overlayer. Oscillatory and chaotic kinetic regimes are found in the simulations. The mechanism of kinetic chaos on the nm scale is shown to be unique compared to that proposed for reactions on single-crystal surfaces.

PACS number(s): 82.65.Jv, 05.45.−a, 68.35.Rh

Simulations of surface reactions are usually performed assuming the adsorbed overlayer to be infinite [1]. Meanwhile, practically important catalytic reactions often occur [2] on very small ($\sim$10 nm) supported crystalline metal particles (for a review of modern nanofabrication technologies, see Ref. [3]). The understanding of the reaction kinetics on such catalysts is far from complete despite long standing interest. To clarify some basic principles in this field, we have recently treated the effect on the nm-scale reaction kinetics of such factor as reactant supply via the support [4], interplay of reaction kinetics on different facets [5], and adsorbate-induced reshaping of catalyst particles [6]. In all cases, we found unique features of the nm-scale kinetics, deviating from those on extended surfaces. Simulations relating the selectivity of catalytic reactions to the geometry of supported catalyst particles have been published by McLeod and Gladden [7].

In this Rapid Communication, we explore a more intriguing phenomenon, namely, oscillatory and chaotic kinetics resulting from adsorbate-induced surface restructuring (AISR) of one of the facets of a nm particle. The fact that AISR may cause kinetic oscillations is well known from the single-crystal studies [8]. Experimental or theoretical data clarifying the details of oscillatory and chaotic kinetics on nm particles are, however, lacking. Among a few relevant studies, we may mention observations [9] of kinetic oscillations in the H_2-O_2 and CO-O_2 reactions occurring on a Pt tip of a field ion microscope. These reports indicate that the oscillations are accompanied by phase separation on the nm scale, which is presumably connected with AISR. In addition, there are simulations of thermal coupling of local oscillators [10,11]. The mechanism (thermal effects [10] and oxide formation [11]) and details of the mean-field (MF) treatments of oscillations on catalyst particles are in the latter simulations completely similar to those on the infinite surface (i.e., the specifics of oscillations on the nm scale is in fact not analyzed).

As an example, we consider the generic catalytic $A+B_2$ reaction occurring via the Langmuir-Hinshelwood (LH) mechanism: $A_{gas} \rightleftharpoons A_{ads}$, $(B_2)_{gas} \rightarrow 2B_{ads}$, $A_{ads}+B_{ads} \rightarrow (AB)_{gas}$. This reaction mimics the essential behavior of, e.g., CO or hydrogen oxidation on noble metals (A stands for CO or hydrogen, and B_2 for O_2). During the past decade, its kinetics for the infinite surface have been studied in detail (see the seminal paper by Ziff *et al.* [12] and the reviews [13]). We analyze one of the most interesting situations (for justification, see Ref. [5]) when the LH step is fast compared to A and B_2 adsorption, B particles are immobile, and A diffusion is rapid compared to the LH step.

The catalyst particle shape is assumed to be a truncated pyramid, with top and bottom (100) faces and (111) side faces, with the largest (100) facet attached to the substrate. The reaction is considered to be accompanied by restructuring of the (001) facet in analogy with CO oxidation on the single-crystal Pt(100) surface [8]. In the latter case, the (1×1) arrangement of metal atoms on the clean surface is metastable compared to a close packed quasihexagonal (''hex'') arrangement. CO adsorption may, however, stabilize the (1×1) phase. The latter provides a feedback necessary for oscillations, because the rate of oxygen adsorption on the (1×1) patches is much higher than on the ''hex'' patches. The MF and MC simulations of such oscillations (on the infinite surface) are numerous (see the reviews [8] and recent MC simulations [14]). The models proposed can, however, hardly be used for describing spatiotemporal patterns on the nm scale. The reason is that the MF treatments do not describe explicitly the reactant distribution. In MC simulation, there is no problem to calculate the distribution, but in the available MC models, the purely mathematical rules employed to realize the steps related to AISR are far from those prescribed by statistical mechanics. For example, surface diffusion of CO molecules is neglected or considered to be independent of the state of metal atoms. With such prescriptions, well-developed surface phases with atomically sharp phase boundaries are lacking. In contrast, the experiment indicates [15] that the CO-induced (1×1) islands are easily formed on Pt(100) even at very low coverages (0.01–0.05 ML). Atomically sharp phase boundaries have also been observed in the field-ion-microscope measurements [9]. To overcome the limitations of earlier simulations, we treat AISR in terms of the theory of first-order phase transitions by employing a well-defined lattice-gas model [16], which was recently used [17] to analyze kinetic oscillations in the NO-H_2, CO+O_2, and CO-NO reactions on Pt(100). For our present goals, the main ingredients of the model are formulated as follows:

(i) The pyramidal crystallite is replaced by a 101×101 square lattice of metal (M) atoms, where the central 51×51

array of sites mimics the top (001) facet, and the periphery represents the side (111) facets. [In reality, the surface densities and symmetry of arrangements of M atoms on the (111) facets and in two phases on the (100) facet are different, but this effect is of minor importance in the present context.]

(ii) On the central facet, every M atom may be in the stable or metastable state (the terms ''stable'' and ''metastable'' refer to the states which are stable and metastable on the clean surface). The energy difference of these states is ΔE. The nearest-neighbor (nn) M-M interaction is attractive, $-\epsilon_{MM}$ ($\epsilon_{MM}>0$), if the atoms are in the same states, and repulsive, ϵ_{MM}, if the states are different (really, the total nn M-M interactions are of course attractive; the interactions $-\epsilon_{MM}$ and $+\epsilon_{MM}$ introduced describe the deviation from the average value). The next-nearest-neighbor (nnn) interactions are ignored. With this choice of the M-M interactions, the model describes the tendency of substrate atoms to be either all in the stable or all in the metastable state.

(iii) Adsorbed particles are assumed to occupy hollow sites forming a 100×100 lattice (this assumption is not essential, because in the case of adsorption on top sites the model will in fact be the same). On sites belonging to the central facet (these sites form a 50×50 lattice), the adsorption energy of a given particle increases linearly with the number of nn substrate atoms in the metastable state (this is a driving force for the phase separation). In particular, the increase of the adsorption energy of an A or B particle after the transition of one nn substrate atom from the stable to the metastable state is ϵ_{AM} or ϵ_{BM} ($\epsilon_{AM}>0$ and $\epsilon_{BM}>0$), respectively.

(iii) The direct nn A-A and A-B lateral interactions, ϵ_{AA} and ϵ_{BB}, are for simplicity neglected. The nn B-B interaction, $\epsilon_{BB}\geqslant0$, is considered to be repulsive and strong so that there are no nn B-B pairs. The latter is often the case for oxygen adsorption on close-packed faces of Pt at UHV conditions.

(iv) The energy of A particles on the peripheral facets is for simplicity set to zero (as in the case of the unrestructured central facet). The relative energy of B particles on the peripheral facets is irrelevant for the analysis, because B diffusion is neglected.

To simulate the reaction kinetics, we use the following set of parameters (with $k_B=1$): $\Delta E/T=2$, $\epsilon_{MM}/T=0.5$, and $\epsilon_{AM}/T=\epsilon_{BM}/T=2$ (such values are typical for surface restructuring). In addition, we introduce the dimensionless parameters, p_{res} and p_{rea} ($p_{res}+p_{rea}\leqslant1$), characterizing the relative rates of surface restructuring, adsorption-reaction steps, and diffusion of A particles. The rates of these processes are considered to be proportional to p_{res}, p_{rea}, and $1-p_{res}-p_{rea}$, respectively. In real systems, surface restructuring is usually slow compared to the adsorption-reaction steps (i.e., $p_{res}\ll p_{rea}$), which are in turn slow compared to A diffusion (i.e., $p_{res}+p_{rea}\ll1$). In our simulations, we employ $p_{res}/(p_{res}+p_{rea})=0.1$ (this means that the reaction is about ten times faster compared to restructuring). In addition, we use the number $N_{dif}\equiv(1-p_{res}-p_{rea})/(p_{res}+p_{rea})$ characterizing the ratio of the rates of A diffusion and the other processes. The results are presented for $N_{dif}=10$.

In our model, the catalytic cycle includes A and B_2 adsorption, A desorption, and the LH step resulting in AB formation. To simulate these steps, we introduce the dimensionless parameters p_A and p_{B_2} for A and B_2 adsorption and p_{des} for A desorption. The rates of these processes are assumed to be proportional to p_A, p_{B_2}, and p_{des}, respectively. The reaction rate between nn A and B particles is considered to be proportional to $1-p_{des}$. For CO oxidation on Pt and in many other reactions, the LH step is much faster than the other steps (except A diffusion), i.e., we should have $p_A+p_{B_2}+p_{des}\ll1$. In our work, we employ $p_A+p_{B_2}=p_{des}=0.05$.

The MC algorithm for simulating the reaction kinetics on the central facet is as follows:

(1) A random number ρ ($\rho\leqslant1$) is generated. If $\rho<p_{rea}$, an adsorption-reaction trial is realized [item (2)]. For $p_{rea}<\rho<p_{rea}+p_{res}$, an attempt of surface restructuring is executed [item (3)]. If $\rho>p_{rea}+p_{res}$, an A-diffusion trial is performed [item (4)].

(2) An adsorption-reaction attempt contains several steps. (i) An adsorption site is chosen at random. (ii) A new random number ρ' is generated. (iii) If the site selected is vacant, A or B_2 adsorption acts are realized provided that $\rho'<p_A$ and $p_A<\rho'<p_A+p_{B_2}$, respectively. For B_2 adsorption, one of the nnn sites is chosen at random, and the trial is accepted provided that these sites have no nn sites occupied by B particles and at least one of the nn M atoms is in the metastable state. The latter means that B_2 dissociation on perfect stable patches is ignored [because the O_2 sticking coefficient on the ''hex'' Pt surface is several orders of magnitude lower compared to that on the (1×1) surface]. (iv) If the site selected is occupied by A, A desorption or reaction act is realized for $\rho'<p_{des}$ and $\rho'>p_{des}$, respectively. For A desorption, a new random number ρ'' is generated and the attempt is accepted if $\rho''<W_{des}$, where $W_{des}=\exp(-\epsilon_{AM}\Sigma_i n_i^M/T)\leqslant1$ is the normalized desorption probability (Σ_i means summation over nn pairs and $n_i^M=1$ or 0 corresponds to the metastable and stable states of nn M atoms, respectively). For A reaction, one of the nn sites is chosen at random, and the trial is fulfilled if the latter site is occupied by B.

(3) For surface restructuring, a M atom chosen at random tries to change its state according to the standard Metropolis (MP) rule [$W=1$ for $\Delta\mathcal{E}\leqslant0$, and $W=\exp(-\Delta\mathcal{E}/T)$ for $\Delta\mathcal{E}\geqslant0$, where $\Delta\mathcal{E}$ is the energy difference of the final and initial states].

(4) For A diffusion, an adsorption site is chosen at random. If the site is vacant or occupied by B, the trial ends. Otherwise, an A particle located in this site tries to diffuse. In particular, an adjacent site is randomly selected, and if the latter site is vacant, the A particle jumps to it with the probability also prescribed by the MP rule.

The MP dynamics is chosen for steps (3) and (4) because this is the simplest dynamics compatible with the detailed balance principle. If necessary, one can easily implement other dynamics for these steps. At present however there are no strong arguments in favor of other rules.

After the specification above, we have only one governing parameter, p_A, by which the relative impingement rates (gas-phase mixture) can be varied. For the separate central

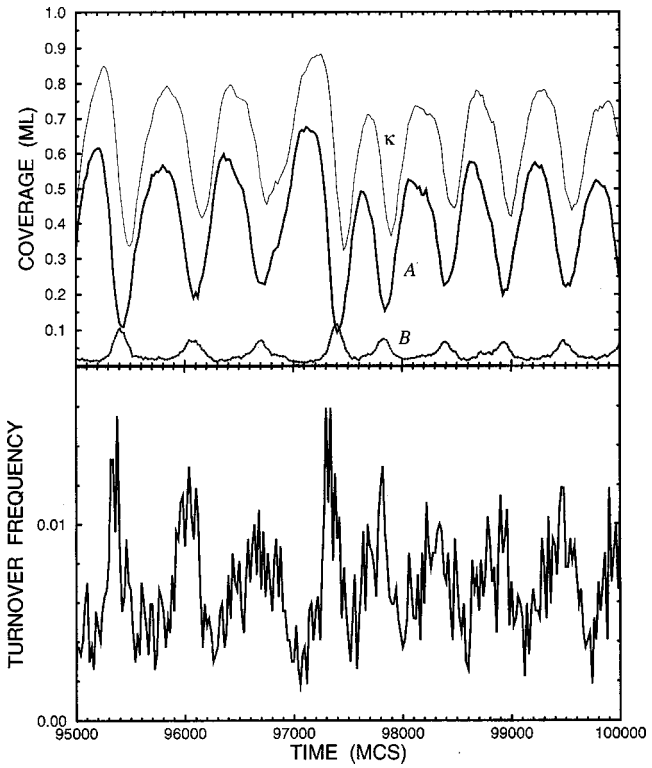

FIG. 1. A and B coverages, fraction of M atoms in the metastable state, κ, and reaction rate (in AB molec. site^{-1} MCS^{-1}) as a function of time for reaction on the separate central facet with $p_A = 0.013$. Time is measured in MC steps (one MCS is defined as 50×50 attempts of the adsorption-reaction-surface-restructuring events).

50×50 facet, the well-developed oscillatory kinetics were found at $0.01 \leqslant p_A \leqslant 0.014$ (Figs. 1 and 2). The amplitude of oscillations is large (e.g., $\simeq 0.3$ ML for A coverage). The large-scale changes in adsorbate coverages are accompanied by small-scale fluctuations with the amplitude comparable with that predicted by the Poissonian distribution (according to this distribution, the amplitude of fluctuations of A coverage is, e.g., expected to be about 0.01 ML). The fluctuations in the reaction rate are larger (because the rate depends on the distribution of both reactants). [With increasing the facet size (e.g., up to 500), the oscillations become more regular as expected for a single-crystal surface. With decreasing the facet size (e.g., down to 20), the oscillations become more chaotic.]

With the results (Figs. 1 and 2) for the isolated central facet, it is now interesting to see how ''communication'' (by diffusion of A) with the peripheral (111) facets will affect the reaction kinetics. In our model, adsorbate-induced surface restructuring occurs only on the central (100) facet. The peripheral (111) facets are stable. The reaction kinetics on the latter facets is assumed to be conventional (no oscillations). Physically, it is clear that in this case the interplay of the reaction kinetics on different facets may weaken or even suppress oscillations on the central facet. Our simulations show, however, that the amplitude of oscillations may still be large and in addition may exhibit qualitatively new features.

For example, let us consider one of the conceptually simplest cases when (i) A adsorption, desorption, and diffusion are realized on the peripheral facets with the same MC rules

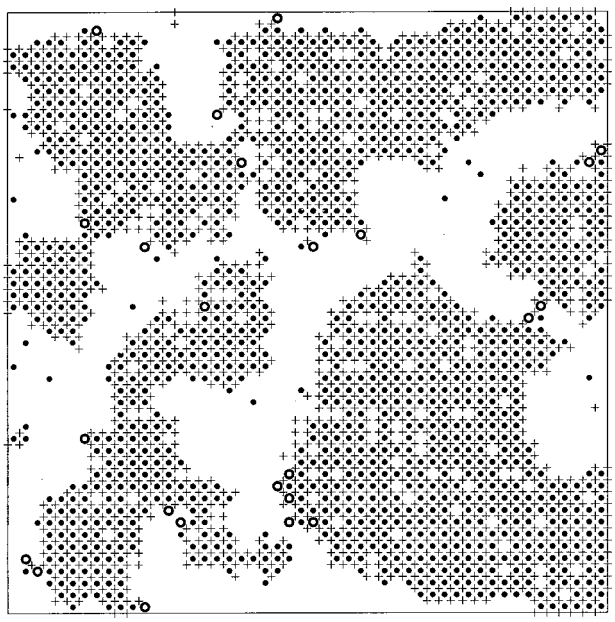

FIG. 2. Typical snapshot of the central facet during the MC run shown in Fig. 1. Pluses correspond to M atoms in the metastable states (M atoms in the stable state are not shown). Filled and open circles exhibit A and B particles adsorbed at hollow sites.

as on the perfect central facet and (ii) B_2 adsorption on the peripheral facets is negligible (due to the low sticking probability). In this case, the main role of the peripheral facets is to provide additional supply of A particles to the central face via adsorption and surface diffusion. This supply shifts the oscillation window to lower p_A values (Figs. 3 and 4) and results in a strongly nonuniform phase distribution on the

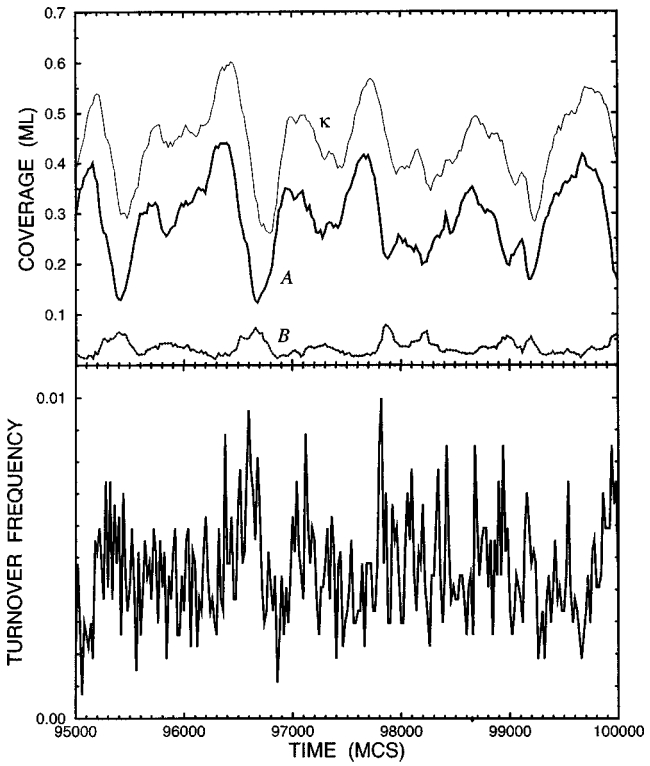

FIG. 3. Chaotic reaction kinetics for the nm particle with communicating facets at $p_A = 0.005$.

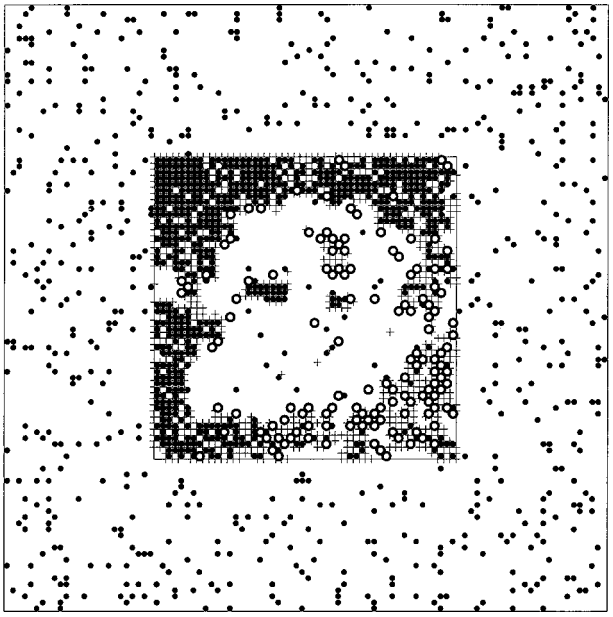

FIG. 4. Typical snapshot of the central and peripheral facets during the MC run shown in Fig. 3. The designations are as in Fig. 2.

central facet (the facet is restructured primarily near the boundaries). In this case, the conditions for oscillations on different regions of the central facet are quite different. In other words, the system possesses a wide distribution of the oscillation frequencies (in addition, the kinetics become very sensitive with respect to small fluctuations in adsorbate coverages). The important point is that different regions are strongly interconnected via adsorbate diffusion. These special features taken as a whole result in chaos in oscillations (Fig. 3). Such chaos, connected with the interplay of the reaction kinetics on adjacent (100) and (111) facets, seems to be inherent for reactions on nm particles and can hardly be observed in reactions on single-crystal surfaces. [Note that in studies of CO oxidation on singly-crystal surfaces of Pt the kinetic chaos was observed [8] only on the (110) face. The nm particles, however, usually do not contain (110) facets.]

Finally, it is appropriate to note that in reality *A* diffusion is much faster than in our simulations. Our results are nevertheless relevant because in our case the *A* diffusion length during the characteristic time of oscillations is much larger than the size of the patterns. This means that the observed pattern formation is primarily connected with surface restructuring (*A* molecules are located mainly inside the metastable patches due to the higher adsorption energy there). Thus, further increase of the *A* diffusion rate is not expected to change the results [for related simulations confirming the latter conclusion, see Ref. [17(b)].

In summary, we have presented MC simulations explicitly illustrating that catalytic reactions occurring on a single nm particle may exhibit oscillatory regimes. Oscillations may be more or less regular or chaotic. On the macroscopic scale, observation of such oscillations may be hampered if synchronization of oscillations on different particles is not effective. All these findings extend the conceptual basis of heterogeneous catalysis.

[1] H.C. Kang and W.H. Weinberg, Chem. Rev. **95**, 667 (1995).
[2] J.M. Thomas and W.J. Thomas, *Principles and Practice of Heterogeneous Catalyst* (VCH, Weinheim, 1997).
[3] G.A. Somorjai *et al.*, Catal. Rev. Sci. Eng. **39**, 77 (1997); B. Kasemo *et al.*, Faraday Discuss. **105**, 237 (1997).
[4] V.P. Zhdanov and B. Kasemo, J. Catal. **170**, 377 (1997).
[5] V.P. Zhdanov and B. Kasemo, Surf. Sci. **405**, 27 (1998).
[6] V.P. Zhdanov and B. Kasemo, Phys. Rev. Lett. **81**, 2482 (1998).
[7] A.S. McLeod and L.F. Gladden, J. Catal. **173**, 43 (1998).
[8] R. Imbihl and G. Ertl, Chem. Rev. **95**, 697 (1995); M. Gruyters and D.A. King, J. Chem. Soc., Faraday Trans. **93**, 2947 (1997).
[9] V. Gorodetskii *et al.*, Nature (London) **370**, 276 (1994); Yu. Suchorski *et al.*, Surf. Sci. **405**, L477 (1998).
[10] F. Schüth *et al.*, J. Chem. Phys. **92**, 745 (1990).
[11] F. Qin and E.E. Wolf, Ind. Eng. Chem. Res. **34**, 2923 (1995).
[12] R.M. Ziff *et al.*, Phys. Rev. Lett. **56**, 2553 (1986).
[13] J.W. Evans, Langmuir **7**, 2514 (1991); V.P. Zhdanov and B. Kasemo, Surf. Sci. Rep. **20**, 111 (1994); E. Albano, Heterog. Chem. Rev. **3**, 389 (1996).
[14] O. Kortüke *et al.*, Phys. Rev. Lett. **83**, 3089 (1999); R.J. Gelten *et al.*, J. Chem. Phys. **108**, 5921 (1998) and references therein.
[15] P.R. Norton *et al.*, J. Chem. Phys. **79**, 3529 (1983); D.A. King *et al.*, J. Chem. Soc., Faraday Trans. **92**, 4781 (1996).
[16] V.P. Zhdanov and B. Kasemo, J. Stat. Phys. **90**, 79 (1998).
[17] (a) V.P. Zhdanov and B. Kasemo, Appl. Cat. A **187**, 61 (1999); (b) V.P. Zhdanov, Phys. Rev. E **59**, 6292 (1999); (c) Surf. Sci. **426**, 345 (1999); (d) J. Chem. Phys. **110**, 8748 (1999).